J. Wind Eng. Ind. Aerodyn. 133 (2014) 124–134

Contents lists available at ScienceDirect

Journal of Wind Engineering and Industrial Aerodynamics

journal homepage: www.elsevier.com/locate/jweia

Effect of low-rise building geometry on tornado-induced loads

Jeremy Case [a,1], Partha Sarkar [b,*], Sri Sritharan [c]

[a] Stanley Consultants, Inc., Muscatine, Iowa, USA
[b] Department of Aerospace Engineering, 2271 Howe Hall, Iowa State University, Ames, Iowa 50011, USA
[c] Department of Civil, Const. and Env. Engineering, Iowa State University, Ames, Iowa, USA

ARTICLE INFO

Available online 28 February 2014

Keywords:
Tornado effects
Wind loads
Laboratory simulation
Low-rise buildings
Building geometry
Tornado-resistant design

ABSTRACT

Despite the destructive effects of tornadoes, limited attempts have been made to quantify tornado-induced loading. The purpose of the study presented here was to investigate the effect of different building geometry on the forces and pressures that low-rise buildings would experience in a simulated tornado with a swirl ratio comparable to what has been measured and recorded for full-scale tornadoes. Measured force and pressure data were then used to judge whether tornado-resistant design for residential structures is feasible. The tornado-induced wind loads were measured on scaled models of buildings in a laboratory-simulated tornado with a core diameter (56 m) and relatively high swirl ratio (2.6) representing an EF3 tornado. The study found that the peak loads vary as a function of eave height, roof pitch, aspect ratio, plan area, and other differences in geometry such as the addition of a garage, roof overhang and soffit. The required strengths of the roof-to-wall and roof sheathing-to-rafter connections were calculated based on the measured loads and compared with their capacities to assess the possibility of failure. It appears that the design of the two critical roof connections in residential construction for tornado-resistant design up to and including EF3 tornadoes can ensure adequate safety cost-effectively by using currently available technology.

1. Introduction

Various opinions as to whether tornado-resistant design of residential buildings is possible, let alone feasible, have been offered. These opinions have been largely motivated by experience obtained from evaluating structural failure due to strong winds and prejudiced by the awe-inspiring destructive capacity of tornadoes, but they have not been based on the comparison of pressure data obtained from either full-scale or laboratory simulated tornadoes with the capacities of the structural connections and members of typical residential construction. Modern engineering is based on the application of rational and empirical principles, but for tornado-resistant design, there has been little or no data that could be used to form engineering principles. In the past, quantification of pressures on a building envelope and forces on a building structure due to the occurrence of a tornado in its proximity has been limited to forensic investigation and engineering judgments. The reason for this limitation is threefold: the lack of research facilities capable of determining the pressures and forces on structures due to tornadoes; the absence of full-scale data to corroborate the results from laboratory experiments or field structures; and a lack of interest in pursuing tornado-resistant design on the part of many as it was assumed to be cost prohibitive.

A tornado simulator has been constructed at Iowa State University (ISU) to overcome the first challenge (Haan et al., 2008). The ISU tornado simulator is capable of creating a model scale tornado that allows building models to be placed in its path as well as having the ability to travel relative to a building model to be investigated. The ISU tornado simulator also has mechanisms to adjust several different variables resulting in different types of tornadoes. The second challenge has also been overcome recently with full-scale data obtained from several recent tornadoes (Karstens et al., 2010; Lee and Wurman, 2005; Wurman, 2002). Subsequent effort has enabled the characteristics of the laboratory simulated tornadoes generated by the Iowa State University (ISU) simulator to be compared with both full-scale data and with computational fluid dynamic models (Sarkar et al., 2005). Work by Thampi et al. (2011) has verified that when the pressures on low-rise building models obtained from a tornado simulated by the ISU simulator are input into a finite element model of a structure, the damage experienced by the corresponding full-scale building in a tornado can be replicated. These advancements

* Corresponding author.
E-mail addresses: CaseJeremy@stanleygroup.com (J. Case), ppsarkar@iastate.edu (P. Sarkar), sri@iastate.edu (S. Sritharan).
[1] Former Graduate Research Assistant, Iowa State University, USA.

http://dx.doi.org/10.1016/j.jweia.2014.02.001
0167-6105

enable determination of forces and pressures on a structure and the exploration of cost-effective solutions for tornado-resistant design.

This paper presents the results of a study that determined the variation of tornado-induced pressures and forces as a function of the geometry and orientation of the low-rise building. In addition, the uplift load capacities of two of the most vulnerable roof connections in light-framed wood construction, as obtained from the literature, in the context of tornado-induced loads based on tornado-induced pressures measured in the laboratory were studied to investigate the viability of tornado-resistant design.

2. Description of simulated tornado

Pressures on low-rise building models obtained from a tornado simulated in a laboratory are useful for investigating the viability of tornado-resistant design only to the extent that the simulated tornado possesses the characteristics of possible full-scale tornadoes. For the purpose of obtaining pressures and forces for the structural design of low-rise buildings, the most important characteristics to reproduce are those that influence the loading on the structure. According to Haan et al. (2010), these characteristics include maximum horizontal wind speed, radius of the core of the tornado and its path, swirl ratio, and translation speed.

2.1. Maximum horizontal wind speed

Based on forensic evidence, around 90% of all tornadoes are rated F2 or less (Bluestein and Golden, 1993). In the EF (Enhanced Fujita) scale (TTU, 2004) this corresponds to an upper bound EF3 tornado, which is estimated to have a maximum velocity of 74 m/s (3-s gust). The design wind speed for the south-eastern and gulf coasts of the United States for occupancy category II buildings per ASCE 7-10 (2010) ranges from 63 m/s to 80 m/s and the basic design wind speed for the same region per the International Residential Code ranges from 54 m/s to 63 m/s (ICC, 2012). The design requirement for straight-line wind speeds of this magnitude implies that design for these wind speeds is possible. Based on the fact that building codes require the design of low-rise building structures for wind speeds of similar magnitudes and that most tornadoes are considered to have maximum wind speeds of 74 m/s or less, the target full-scale horizontal wind speed for this study of tornado-induced loads was chosen to be 74 m/s.

The maximum tangential velocity of the tornado generated by the ISU Tornado Simulator in this study was measured to be 11.6 m/s at a height of 19 mm and a maximum horizontal velocity of 11.7 m/s at the same height. Using a full-scale tornado with a maximum horizontal velocity of 74 m/s (EF3) gives a vortex velocity scale of $\lambda_V = 11.7/74 = 1/6.3$ for a full-scale averaging time equivalent to the model-scale averaging time. A contour plot of the tangential velocity normalized with the maximum tangential velocity is shown in Fig. 1.

2.2. Tornado vortex diameter

Brooks (2004) conducted a study using reported tornado damage path lengths and widths to model Weibull distributions of Fujita scale levels. The distributions produced by the study showed the probability of a tornado path width, given the occurrence of a tornado at a specific Fujita scale intensity. This study showed that a tornado's mean path width increased with its Fujita scale rating. According to Brooks for a F1 or a F2 tornado (corresponding approximately to an EF2 or EF3 tornado), the path would be most likely between 100 and 500 m.

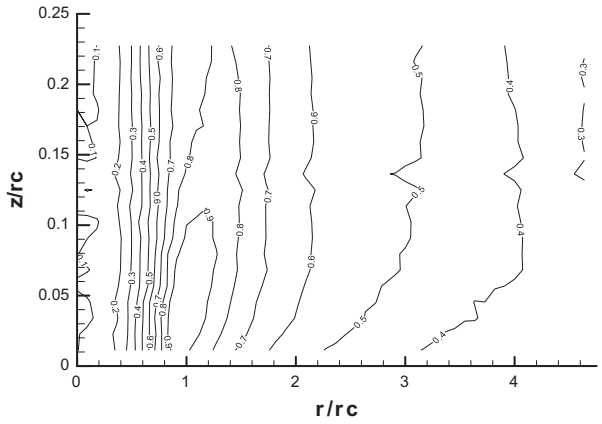

Fig. 1. Contour plot of tangential velocity magnitudes normalized with respect to the maximum tangential velocity.

Assuming that damage occurs at the design wind speed specified in the building codes, which for the Midwestern United States is 40 m/s, and the full-scale horizontal velocity is 74 m/s (EF3), the damage to buildings and other structures may be expected to occur within a diameter where the horizontal wind speed exceeds approximately half of the maximum tangential wind speed. The "0.5" contour in Fig. 1 is located at 2.2 times the radius of the maximum wind (radius of the core) near the ground. According to the results of the study conducted by Brooks (2004), the radius of the core of an EF3 tornado would have a high probability of being between 45 and 225 m. The radius of the core for the simulated tornado used in the study presented here was 0.56 m, which matches with the study done by Brooks (2004) when scaled using a length scale of 1:100.

2.3. Swirl ratio

One of the most commonly used parameters for laboratory and numerically simulated tornadoes is the swirl ratio (Haan et al., 2008; Hangan and Kim, 2008). The swirl ratio (S) is the ratio of the tangential momentum to the inflow rate (Q) of the vortex measured at a particular radius ($S = \pi V_{\theta max} r_c^2/Q$, r_c is core radius where maximum tangential wind speed $V_{\theta max}$ occurs). Several studies have shown that the swirl ratio is the parameter that governs the flow characteristics of a tornado (Hangan and Kim, 2008; Church et al., 1979). Davies-Jones (1973) demonstrated that the radius of the vortex core is a function of the swirl ratio. Both Davies-Jones (1973) and Church et al. (1979) showed that the vortex structure is related to the swirl ratio; as the swirl ratio increases the vortex breaks down into multiple vortices (Davies-Jones, 1973).

The data from full-scale tornadoes indicate swirl ratio values of 2.0 or greater. For example, when comparing the full-scale data from the Spencer, South Dakota, tornado with 3D numerical simulations Hangan and Kim (2008) found that the best fit was for a swirl ratio of $S = 2$. Using data obtained with a Doppler on wheels (DOW), the swirl ratios of the Mulhall tornado were calculated by Lee and Wurman (2005) to be between 2 and 6 for the F4 level tornado. These swirl ratios were measured at the radius of the vortex core (r_c). Based on the latest data obtained by DOW and the best fit of that data with numerical results, it was decided that an attempt should be made to increase the swirl ratio of the tornado used in this study to a value of 2 or greater. In the ISU tornado simulator, a 1.83 m (6 ft)-diameter fan creates an updraft. The flow is then directed downward through concentric ducts. Rotational flow is created by several vanes fixed at a given angle with respect to the radial direction that is normal to the tangent of the duct. The swirl ratio of the vortex generated in the Iowa State University's tornado simulator can be increased by

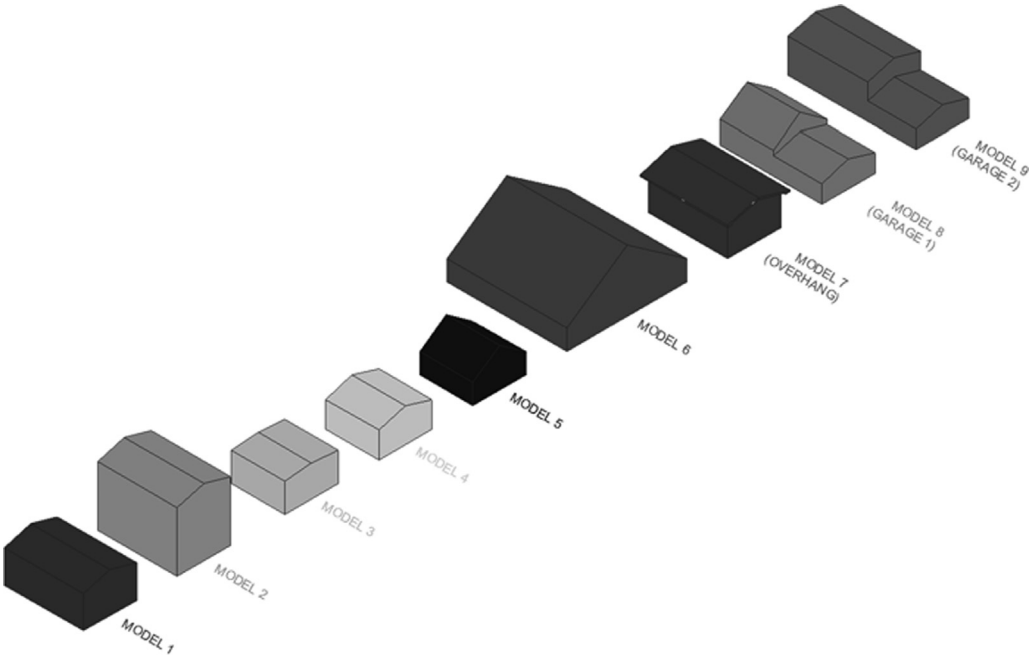

Fig. 2. Building models used in the study.

increasing the vane angle (Haan et al., 2008). In order to obtain a high swirl ratio the vane angle was set at 75°, resulting in a swirl ratio of 2.6 measured at the core radius or radius of the maximum tangential velocity.

2.4. Translation speed

Various translation speeds of full-scale tornadoes have been reported: 16.5 m/s (Thampi et al., 2011), 13 m/s (Lee and Wurman, 2005) and 23 m/s (Haan et al., 2008). Based on these reports, pressure measurements on the building models in this study were taken for a tornado translation speed of 0.15 m/s. If it is assumed that damage to a building is proportional to the duration of its exposure to the tornado winds then the vortex translation time scale (λ_T) should be equal to one. This results in vortex translation velocity scale equal to the length scale used in modeling. Thus, the translation speed of 0.15 m/s at model scale becomes 15 m/s at full-scale for a length scale (λ_L) of 1:100.

2.5. Surface roughness

The ground plane was varnished plywood which was very smooth. No surface roughness blocks were used and therefore this plane represented an open terrain. Since much of "Tornado Alley" is rural farmland, open terrain was considered to be a valid and useful exposure to use in the study.

3. Model description, instrumentation, and conventions

3.1. Building models

External surface pressure measurements were taken on nine building models (Fig. 2) with gable type roofs with varying roof pitches (4.6–35.5°), eave heights (12.2–36 ft), L/B ratios (1.0 and 1.5; where L is the length and B is the width)) and h/L ratios (0.34–0.8; where h is the mean roof height), attached garage (with and without) and a variety of test cases (154 total) were conducted that included varying the building orientation angles with respect to the path of the tornado. Each model was fitted with as many as 124 pressure taps.

Model dimensions were selected such that when scaled using a length scale of 1:100 the models would have realistic low-rise building dimensions and also the effect of roof height, aspect ratio, roof pitch, overhang and an attached garage on the external pressures and forces due to the simulated tornado could be observed. The selection of the dimensions was based on commonly available, simple house plans and a table similar to Fig. 6-6 in ASCE 7-10 (2010), where roof pressure coefficients are tabulated as functions of mean roof height divided by the length of the building, wind direction and roof pitch. The model dimensions are given in Table 1.

3.2. Instrumentation

Wind velocity measurements while the simulator was stationary were taken at 78.1 Hz for 26 s with a Cobra probe (multi-hole probe, TFI®). Measurements were taken at points spaced at 50.8 mm horizontally and 6.35 mm vertically. The measurements were taken starting at an elevation of 6.35 mm until an elevation of 127 mm and for a horizontal length of 2.64 m at each elevation from the ground plane.

Pressure measurements were taken using two high-speed 64-channel ZOC33/64Px pressure transducers (Scanivalve Corporation®) at a frequency of 390 Hz. The static pressure used in both the pressure and the velocity measurements was taken as the laboratory ambient pressure under the ground plane.

3.3. Procedure and conventions

For each test case the pressures were recorded 10 times. The peak pressures were calculated as the average of the peak pressures from each of the 10 runs. The orientation of the building (building orientation angle, BOA) with respect to the direction of translation of the tornado (Fig. 3) was varied from 0° to 90° with a step size of 15°. The 0° orientation corresponds to the direction of translation of the tornado being parallel to the ridge of the roof of the building model (along dimension L). The garage models were tested from 0° to 90° (Orientation 1) and from 180° to 270°

Table 1
Model dimensions.

Model	Roof pitch, θ (deg)	Width, B (mm)	Length, L (mm)	Eave height, h_e (mm)	Roof ridge height, h_t (mm)	Mean roof height, h (mm)	L/B	h/L
1	15.95	98	146	60	74	67	1.5	0.46
2	15.95	98	146	110	124	117	1.5	0.80
3	4.6	98	98	53	57	55	1.0	0.56
4	15.95	98	98	48	62	55	1.0	0.56
5	35.5	98	98	37	72	55	1.0	0.56
6	35.5	221	221	37	114	76	1.0	0.34
7 (Overhang)	15.95	98	146	60	74	67	1.5	0.46
8 (Garage 1)[a]	35.5[b]	98	187	37	72	55	1.9	0.29
9 (Garage 2)[a]	15.95[b]	98	235	60	74	67	2.4	0.29

[a] Dimensions of "garage" addition were B=98 mm, L=89 mm, h_e=33 mm, and h_t=47 mm.
[b] Roof pitch of "house" part of model. Roof pitch of "garage" addition was 15.95°.

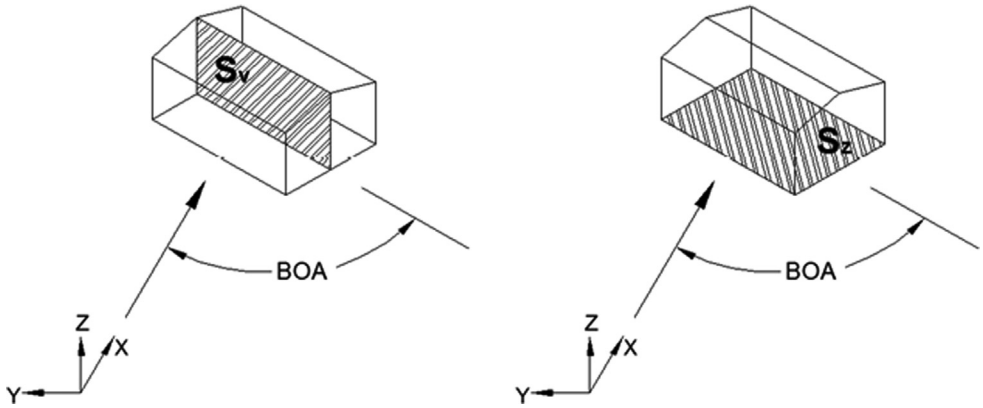

Fig. 3. Building orientation angle (BOA) with respect to the tornado translation axis (X) and areas (S_v, S_z) used to normalize force coefficients.

(Orientation 2). The taller part of the garage models experienced the tornado first for Orientation 1 and the shorter part of the model experienced the tornado first for Orientation 2. For all of the test cases, the tornado translation axis passed through the center of the building model.

The aerodynamic force coefficients were computed along the x (horizontal direction parallel to the tornado's translation direction), y (horizontal direction perpendicular to the tornado's translation direction), and z (vertical) directions. An xy force coefficient (C_{Fxy}) which was computed as the square root of the sum of the squares of the x (C_{Fx}) and y (C_{Fy}) force coefficients was also considered important as a quantity expressing the total drag force on the low-rise building model. The x and y coefficients were normalized with an area of the model (Fig. 3) equal to the height of the ridge of the roof times the length of the roof ridge (S_v). The z coefficient (C_{Fz}) was normalized with an area (Fig. 3) equal to the floor plan of the model (S_z). The equations used to calculate the force coefficients are given as the following equations.

$$C_{Fx} = \frac{F_x}{(1/2)\rho V_H^2 S_v} \quad (1)$$

$$C_{Fy} = \frac{F_y}{(1/2)\rho V_H^2 S_v} \quad (2)$$

$$C_{Fz} = \frac{F_z}{(1/2)\rho V_H^2 S_z} \quad (3)$$

$$C_{Fxy} = \sqrt{C_{Fx}^2 + C_{Fy}^2} \quad (4)$$

4. Results

The peak pressure and force coefficients were calculated and the time histories of the force coefficients were plotted for each of the models for each building orientation angle. The peak pressure and force coefficients and time histories of the different models were then compared to discover any trends that would demonstrate the effect the different geometric variables had on the tornado-induced forces and pressures. Models with geometry that was similar or exactly the same except for one variable were compared in an effort to isolate the effect of each variable.

4.1. The effect of eave height

Models 1 and 2 had the same plan area and plan aspect ratio (L/B), and the same roof slope. The difference between the two models was their eave heights; the eave height of Model 2 (110 mm) was almost twice that of Model 1 (60 mm). For each of the building orientation angles the peak pressure contours of the two models were similar but had different magnitudes. The peak pressures on Model 1 were significantly higher. The eave heights of both models were greater than the height at which the maximum tangential velocity was measured (19.5 mm). The maximum tangential velocity at a height equal to the eave height of Model 1 was 10.6 m/s while the maximum tangential velocity at a height equal to the eave height of Model 2 was only 9.6 m/s. This may help to explain the difference in peak pressures as a function of eave height. The average peak pressure contour plots for the 30° building orientation angle of Model 1 and Model 2 can be seen in Fig. 4. The C_{Fz} and C_{Fxy} time histories of the two models for the 30° building orientation angle can be seen in Figs. 5 and 6, respectively.

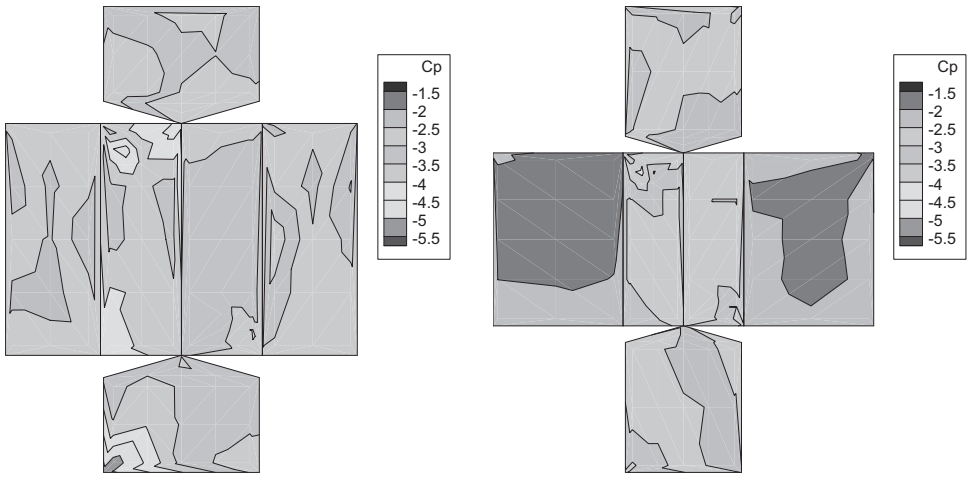

Fig. 4. Peak pressure contours for Model 1 (left) and Model 2 (right) for the 30° building orientation angle.

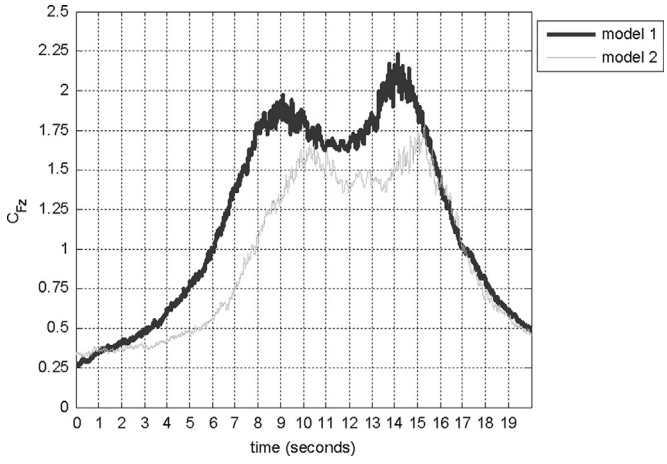

Fig. 5. Vertical force coefficient time history for Models 1 and 2 for the 30° building orientation angle.

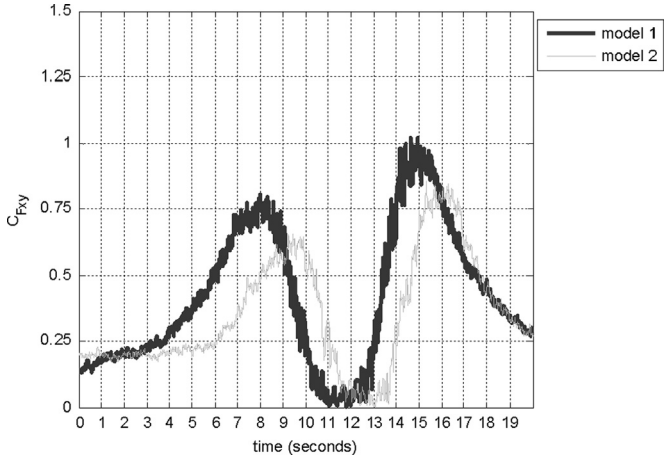

Fig. 6. XY force coefficient time history for Models 1 and 2 for the 30° building orientation angle.

4.2. The effect of roof pitch

Models 3, 4 and 5 were compared to observe how roof pitch affects tornado-induced pressures and forces. All three models had the same mean roof height (55 mm), the same plan dimensions, and the same aspect ratios ($L/B=1.0$ and $h/L=0.56$). Model 3 had a roof pitch of 4.6°, Model 4 had a roof pitch of 15.95° and Model 5 had a roof pitch of 35.5°. A clear trend occurs in the average peak pressures; as the roof slope increases the peak pressure magnitudes for the roof decrease while those for the walls increase. The peak C_{Fz} for Models 3 and 4 occurs for the 45° building orientation angle while for Model 5 the peak C_{Fz} occurs for the 60° BOA. The average peak pressure contour plots for the 45° building orientation angle of Model 3, Model 4, and Model 5 can be seen in Fig. 7.

Haan et al. (2010) found that the peak uplift force resulting from tornado-induced loads does not vary with the building orientation. Fig. 8 confirms this finding and shows that the peak uplift force also did not vary with roof pitch for building Models 3, 4 and 5. The peak pressures can vary while the peak vertical force coefficient may not vary significantly because the peak pressures do not necessarily occur simultaneously at all locations while the peak force coefficients occur when the integration of the instantaneous pressures results in the largest force coefficient.

4.3. The effect of the ratio of plan dimensions

The lower maximum tangential velocity at the eave height of Model 2 as compared with the maximum tangential velocity at the eave height of Model 1 was considered to have caused the difference in peak pressures and vertical force coefficients. Model 4 had the same roof slope as Models 1 and 2, but had an eave height of 48 mm. The maximum tangential velocity at this height was 10.85 m/s, higher than for both Model 1 (10.6 m/s) and Model 2 (9.6 m/s), but the peak C_{Fz}'s for Model 1 are still higher than for Model 4. The most significant difference between Model 4 and Model 1 was the L/B ratio o, often referred to as the building's aspect ratio. The aspect ratio of Model 1 was 1.5 while Model 4's aspect ratio was only 1.0. The fact that the model's aspect ratio is significant to the magnitude of the tornado-induced forces and pressures acting on it can be seen when the C_{Fz} time history of Model 4 in Fig. 9 is compared with the C_{Fz} time history of Models 1 and 2 in Fig. 5. The C_{Fz} time histories of Models 1 and 2 show an initial peak followed by a period of lower values for C_{Fz} then another peak as the last part of the simulated tornado passed over the building. This is different than the C_{Fz} time history of Model 4 which has a period of relatively constant C_{Fz} values while the simulated tornado is directly over the model. An aspect ratio greater than 1 allows the tangential velocity to play a clear role in increasing the peak C_{Fz} values for those models.

Comparison of the C_{Fz} time history of Model 1 in Fig. 5 with the C_{Fz} time history of Model 6 in Fig. 13 gives evidence that the cause of difference in the shape of the C_{Fz} time history was due to the aspect ratio and not the building's overall length. Although the

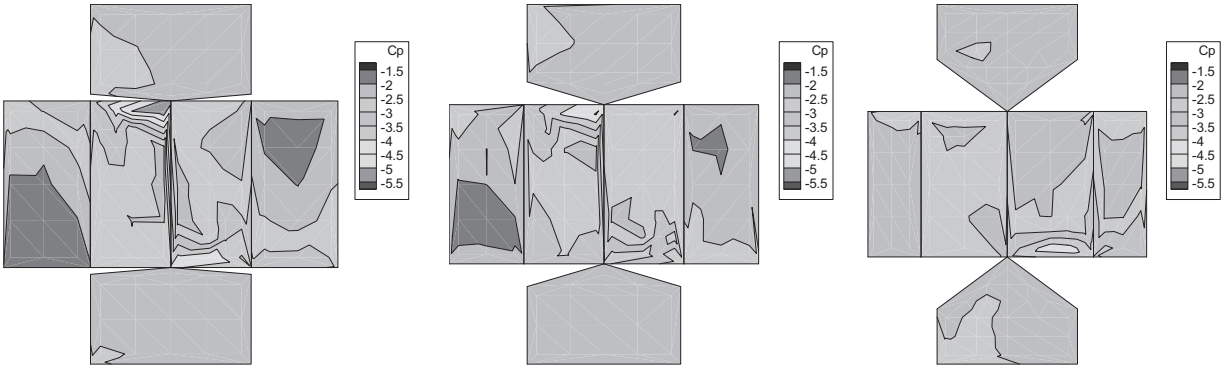

Fig. 7. Peak pressure contours for Model 3 (left), Model 4 (center), and Model 5 (right) for the 45° building orientation angle.

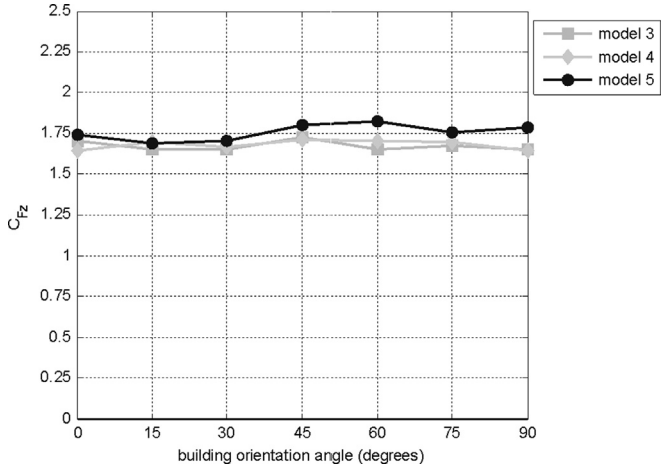

Fig. 8. Peak vertical force coefficients for Models 3, 4 and 5 for each building orientation angle.

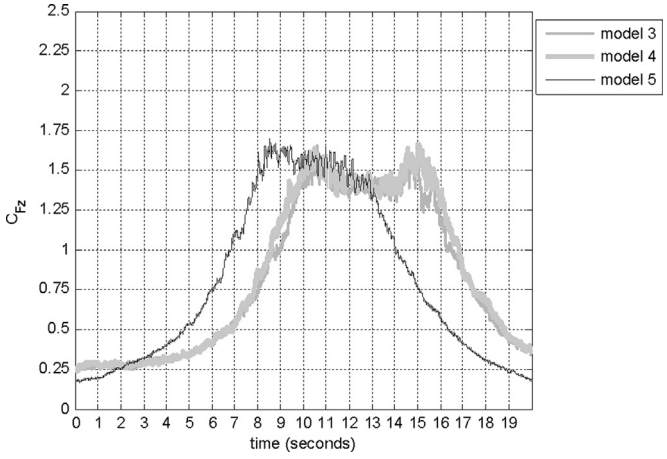

Fig. 9. Vertical force coefficient time history for Models 3, 4 and 5 for the 30° building orientation angle.

length of Model 6 was 221 mm and the length of Model 1 was only 146 mm, the shape of the time history of Model 6 is similar to the other model's with aspect ratios of 1.0.

4.4. The effect of an enclosed overhang and soffit

It was considered important to investigate the effect of an enclosed overhang and soffit on the tornado-induced forces and pressures on low-rise buildings since most low-rise residential buildings in the United States have roofs that extend past the building's walls and many have enclosed soffits. All of the models, except the one which was constructed with a roof overhang and an enclosed soffit (i.e., Model 7 referred to as the "overhang" model), had sharp corners where the roof met the wall. The overhang model was exactly like Model 1 except for the overhang and soffit. Internal pressures were not considered for either model.

Pressures were measured on the underside of the soffit. The peak pressure coefficients for the underside of the soffit ranged from -1.0 to -3.0 depending on the building orientation angle and the region of the soffit. Although the magnitudes of the peak pressures on the overhang model were significantly less than on Model 1, the pressure contour shape on the walls was similar. The distribution of the peak pressure contours on the building walls were less affected by the overhang than those on the roof. Fig. 10 shows the peak pressure contour plots for Model 1 and the overhang model for the building orientation angle of 30°.

Fig. 11 shows how significant the addition of the roof overhang was to the vertical force coefficient. Similar to the peak pressures, the horizontal force coefficients were also less affected by the overhang and soffit than the vertical force coefficients. This is shown in Fig. 12.

4.5. The effect of plan area and height to length ratio

Both Model 5 and Model 6 have a roof pitch (θ) of 35.5°, an eave height (h_e) of 37 mm and an aspect ratio (L/B) of 1.0, but had different plan dimensions, 98 mm and 221 mm respectively and different total heights (h_t), 72 mm and 114 mm respectively. These dimensions resulted in a mean roof height to length (h/L) ratio of 0.34 for Model 5 and 0.56 for Model 6. Model 6 was made so much larger than Model 5 in order to maximize the difference in h/L ratios. The large plan dimension of Model 6 is almost 40% of the radius of the core of the simulated tornado. This results in a significantly longer period in which the building's structure must resist the tornado-induced forces as can be seen in Fig. 13.

4.6. The effect of an attached garage

Most of the residential buildings or houses built in the United States have attached garages. The attached garage is often shorter in elevation and oriented with its roof ridge parallel to the ridge of the roof of the house. Two models with attached "garages" were tested. Model 8 or garage 1 model was an exact replica of Model 5 except with an attached garage. Similarly, Model 9 or garage 2 model was an exact replica of Model 1 except with an attached garage. The dimensions, eave height and roof slope of the "garage" on both models were exactly the same. Similar to the other models, pressures were recorded for the garage models with building orientation angles between 0° and 90° at 15° intervals. This was done twice for each of the garage models: once where

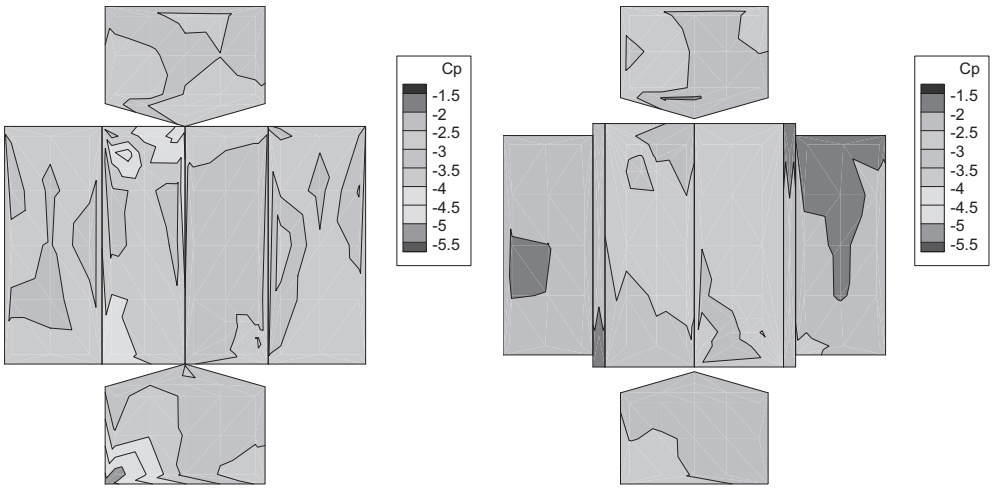

Fig. 10. Peak pressure contours for Model 1 (left) and the Overhang Model (right) for the 30° building orientation angle (Overhang Model – the contours for the long narrow rectangles correspond to the soffit and the contours on the roof include the overhang).

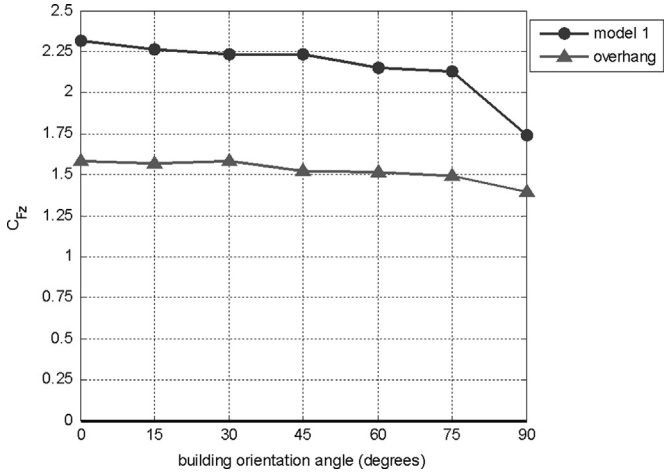

Fig. 11. Peak vertical force coefficients for Models 1 and 7 or overhang model for each building orientation angle.

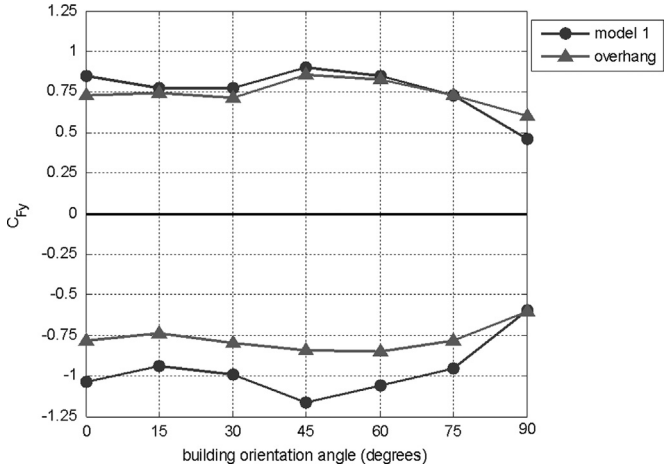

Fig. 12. Peak horizontal, *Y*-direction force coefficients for Models 1 and 7 or overhang model for each building orientation angle.

the simulated tornado struck the "house" part of the model first (Orientation 1) and once where the simulated tornado struck the "garage" part of the model first (Orientation 2).

The addition of the garage increased the plan aspect ratio (L/B) of the original models. The increased aspect ratio of the garage

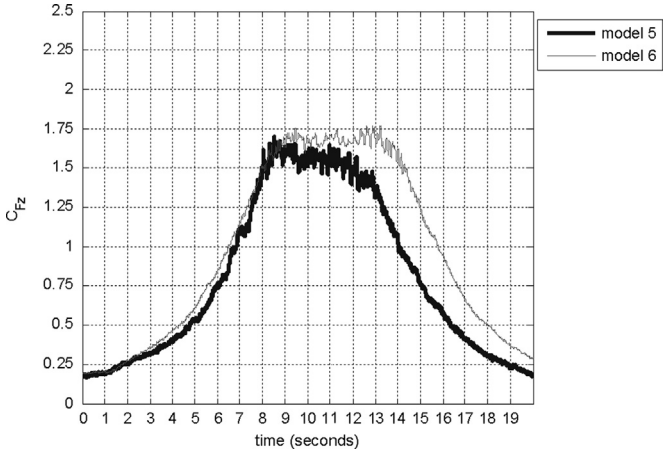

Fig. 13. Vertical force coefficient time history for Models 5 and 6 for the 30° building orientation angle.

1 model resulted in larger peak vertical force coefficients than Model 5 (without a garage) for most building orientation angles. While for the garage 2 model the peak vertical force coefficients were larger than the models with aspect ratios (L/B) of 1.0, but for most building orientation angles they were less than those for Model 1.

The addition of the garage to the models created more complex geometry which resulted in an interaction between the building model and the simulated tornado. The study of this interaction will require the testing of additional models in order to fully understand the effect of the garage addition.

4.7. *The effect of building geometry on roof connection demand*

Although not presented here, a comparison of the peak force coefficients, *X*, *Y* and *Z*, for each of the building models and each building orientation angle revealed that without exception the vertical force coefficient was greater than both of the horizontal force coefficients, sometimes by a factor of 2. The peak pressure coefficients also occurred on the roof for all of the models. Both the peak force and pressure coefficients are negative and act away from the roof, subjecting the structural connections in the roof to uplift forces. This agrees with the findings of Haan et al. (2010).

In light of these findings, it is not surprising that many damage surveys done after tornado events have found that roof damage is one of the most common types of damage to occur in residential

buildings. The occurrence of roof damage is further aggravated by the fact that, for residential construction in the regions of the United States where tornadoes most often occur, the connections in the load path from the surface of the roof to the wall and then to the foundation are almost always nailed. Nailed connections increase the vulnerability of roofs to uplift failure because nails are inherently weak in tension. The loss of the roof increases the vulnerability of the rest of the house, because the exterior walls are composed of diaphragms that are tied together and braced at their tops by the roof structure (Marshall, 2002). Therefore, the roof is vital to the survivability of the house and since the connections in the roof are the weak points in the load path due to the nature of tornado-induced loads great improvements in the ability of low-rise buildings to resist tornado-induced forces could be made by improving these connections.

Sparks et al. (1988) demonstrated that the roof of low-rise buildings is critical to the integrity of the structure and that for straight-line winds failure of roof connections is dependent not only on wind speeds but also on roof geometry. These researchers also noted that failures of entire residential structures can occur quickly after the loss of the roof. Based on their findings, the connection between the roof trusses and the stud walls was considered to be the critical connection for the survival of the entire house (Sparks et al., 1988). In addition to finding that the roof-to-wall connection (RTWC) was the most critical, they found that for several different roof geometries the toe nailed RTWC would fail at wind speeds as low as 54 mph (3-s gust) which is much less than the design wind speed of 90 mph (3-s gust) in boundary layer winds.

The other type of connection in residential roof construction that is susceptible to uplift loads is the connection of roof sheathing to the rafters or roof trusses. The roof sheathing has many structural functions including giving lateral support to the roof framing, acting as a surface to which loads are applied and distributed to the roof framing, and as part of the building envelope to aid in keeping the building sealed so as to prevent the inside of the building from becoming pressurized. These functions are critical to the ability of the residential structure to survive a tornado.

The sequence of progressive failure of low-rise residential structures in tornadoes is not well understood. Thampi et al. (2011) demonstrated that once the building envelope is breached, either through failure due to wind pressures or debris impact, internal pressures change the sequence of failure and failure mode of the structure. Thampi et al. (2011) also demonstrated that the failure of the roof occurred for a sealed building, but the failure of a door caused failure of the gable end. Therefore, for the purpose of tornado-resistant design, it is useful to understand where the initial failure is most likely to occur. Due to the complexity of failure sequences of low-rise buildings in tornadoes, the analysis of the roof connections below was done assuming that the rest of the structure remained intact until the connections failed.

Models 1 and 5 were used in the analysis to compare the tornado-induced load on the roof connection with the capacity of the roof connections as reported in the literature, as well as to observe the difference in load on the roof connections for the two models with different dimensions and roof pitch. The pressure time histories of the two models were first converted to pressure coefficient time histories using Eq. (5), where P is the recorded pressure (i.e. the total pressure minus the static pressure) at time step i, V_H is the average horizontal component of the wind velocity measured at the radius of the core, and ρ is the density of air.

$$C_p = \frac{P_i}{(1/2)\rho V_H^2} \tag{5}$$

4.7.1. Roof sheathing connection

In the field of aerodynamics terms such as “windward”, “leeward”, “leading”, and “trailing” are often used to describe certain parts of an object immersed in a straight-line flow. These terms are not as easily defined for flow in a tornado, but because of a lack of alternatives they will be used in the following discussion. The terms are defined for the sides of the models for a building orientation angle of 0° and counter-clockwise flow. The sides referred to by the terms do not change with the building orientation angle. The conventions used are as follows:

- Windward: The side of the model that experiences the tangential velocity component first and is parallel to the direction of the translation of the tornado.
- Leeward: The side of the model that is parallel to and opposite of the windward side.
- Leading: The side of the model that is perpendicular to the direction of translation and is the closest to the tornado before the tornado reaches the model.
- Trailing: The side of the model that is perpendicular to the direction of translation and is the closest to the tornado after the tornado has passed the model.

For the 0° building orientation angle the peak pressures for Model 1 occurred at the leading, leeward corner and roof edge. For building orientations 15° through 75°, the peak pressures on Model 1 occurred at the trailing leeward roof edge and at the windward leading roof edge while for Model 5 the highest peak pressures occur mainly at the leading, windward roof edge and the leading, windward wall edge. For a building orientation of 90°, the pressures are not as high as for other building orientations and the highest peaks for Model 1 occur in the trailing, windward region of the roof and for Model 5 occur in the leading, leeward region of the roof. The maximum peak pressure coefficient from all building orientation angles for Model 1 is −6.1 and for Model 5 is −4.9.

Using the maximum peak pressure coefficients obtained for Models 1 and 5 and the capacity of roof sheathing as reported in the literature for different types of nails and nailing schedules, the required wind velocity for sheathing panel uplift failure can be determined. The full-scale tornado horizontal wind velocities with the same averaging time as the model-scale tornado required to exceed the capacities of sheathing panels with various fastener types and spacing are shown in Table 2. Simply by using 8d ring shank nails spaced at 150 mm along the edges of the panel as well as in the middle of the panel (150/150), the velocity required to create an uplift pressure using the peak pressure coefficients approaches what is considered an EF3 tornado. Installing 8d ring shank nails with a slightly heavier nailing schedule instead of 6d smooth shank nails has an insignificant cost when compared to the total cost of residential construction. Such a small increase in cost is certainly justifiable if the tragedy caused by tornadoes can be lessened.

Table 2
Required wind velocity for sheathing panel uplift failure.

Nail type	Nailing schedule (mm)	Capacity (kN/m^2)	Velocity required for C_p=6.1 (m/s)	Velocity required for C_p=4.9 (m/s)
8d Smooth shank	150/300	4.6	33.35	37.22
8 d Ring shank	150/300	8.04	46.37	51.74
8d Smooth shank	150/150	7.3	44.18	49.30
8 d Ring shank	150/150	12.5	57.82	64.51

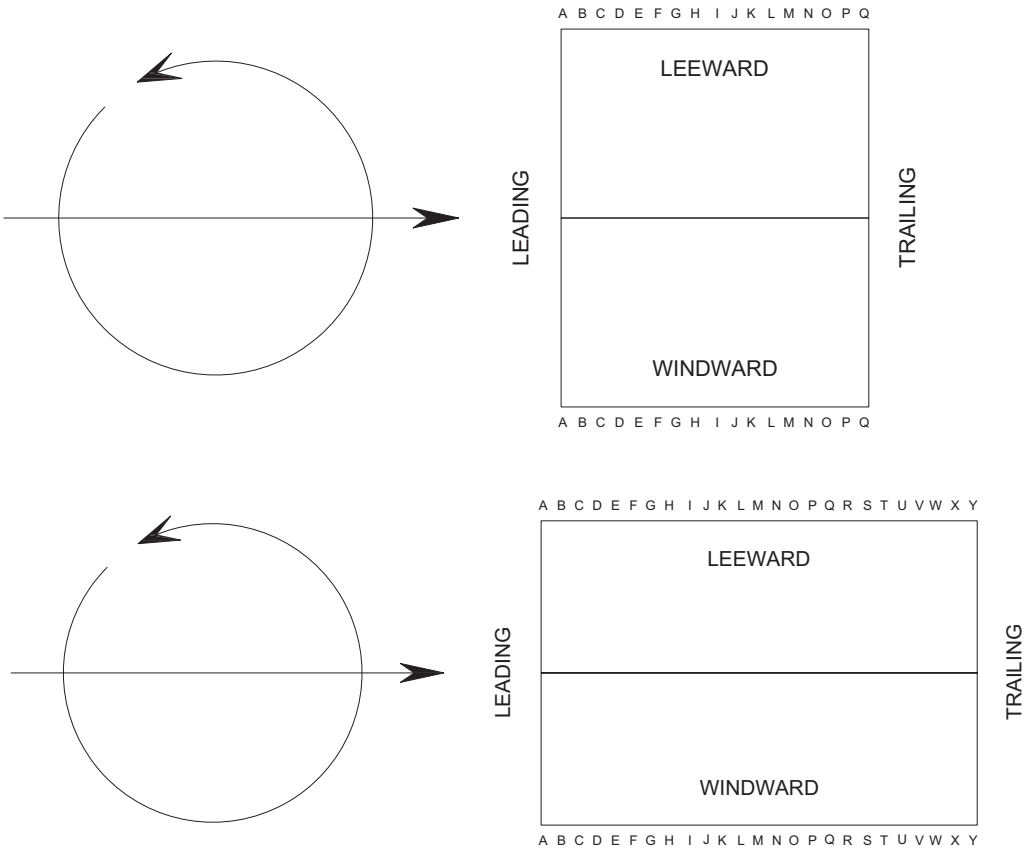

Fig. 14. Location of roof truss connections with respect to the moving tornado for Model 1 (top) and Model 5 (bottom).

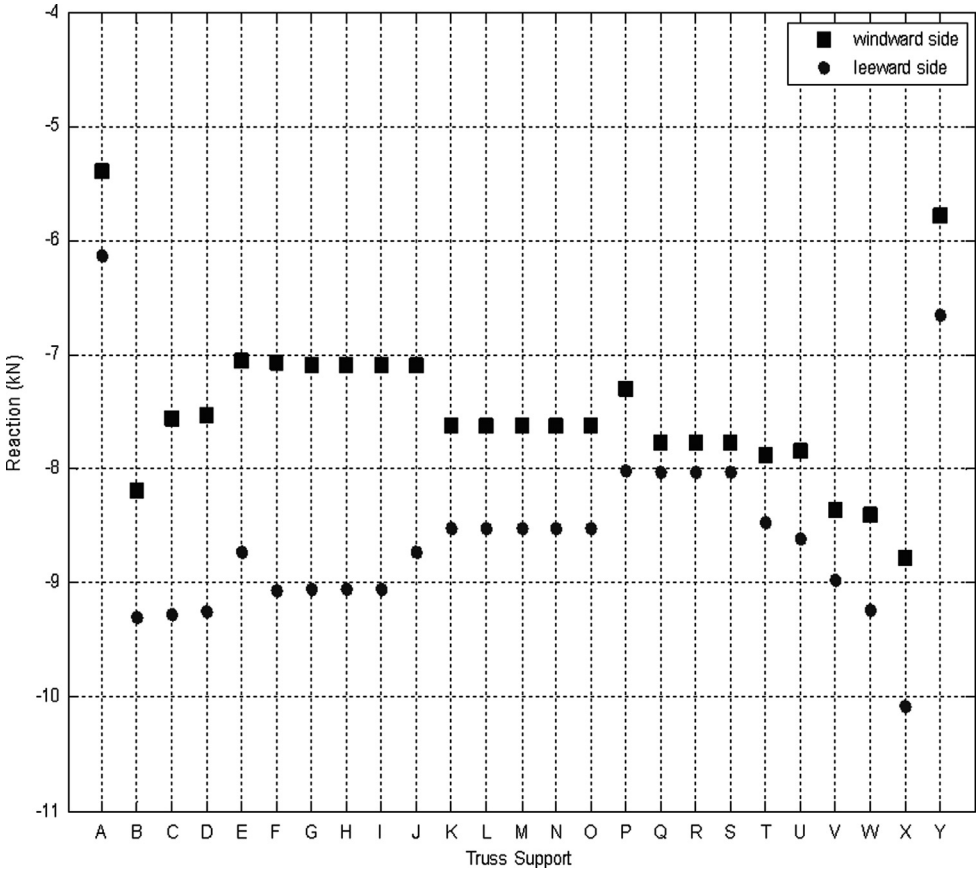

Fig. 15. Peak roof truss reactions for Model 1.

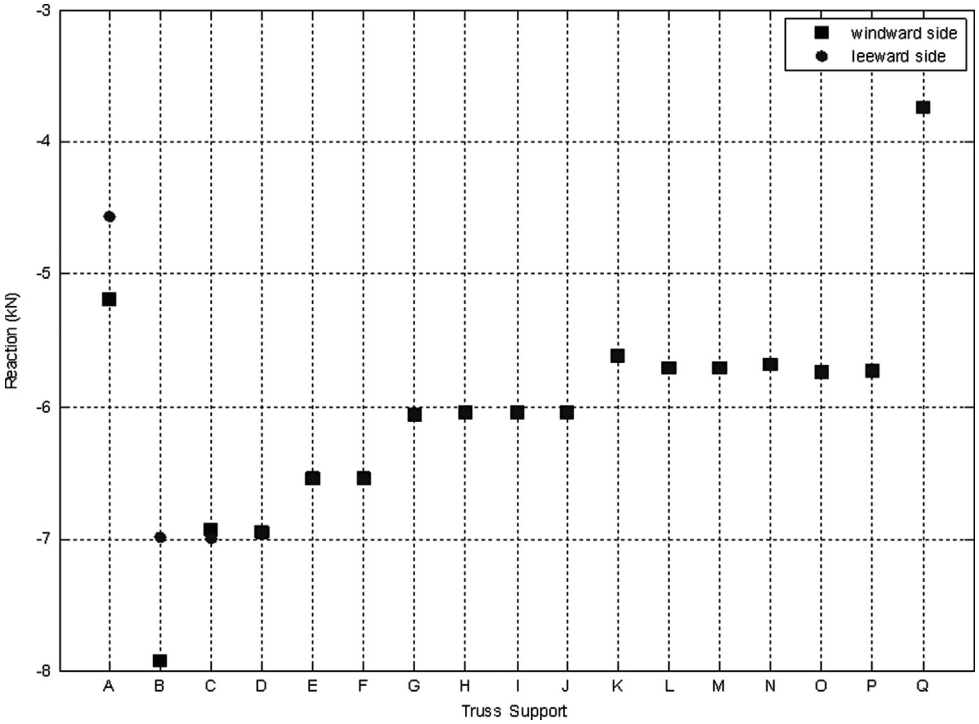

Fig. 16. Peak roof truss reactions for Model 5.

4.7.2. Roof-to-wall-connection

In order to obtain the full-scale roof-to-wall connection reactions, the maximum model-scale horizontal velocity was scaled to a full-scale velocity of 74 m/s based on the assumption that this full-scale velocity has an averaging time equivalent to the averaging time of the model scale. The time scale (λ_T) was then calculated to be 1:15.9 based on the velocity scale (1:6.3) and length scale (1:100).

The dimensions of the models were scaled up to full-scale using a length scale of λ_L=1:100. Spacing of the roof trusses at full-scale was 0.6 m (24 in.) on center. The influence functions for these particular models were not available and were beyond the scope of this study; therefore, rectangular tributary areas were used instead. The pressure tap tributary areas were then laid over the truss tributary areas creating a grid. Each area of the grid corresponded to a particular truss (Fig. 14) and a particular pressure tap. Using the pressure coefficient time histories and Eq. (5) the full-scale pressures were calculated for each area at each time step. In the analysis the pressures were considered to be uniform over their respective areas on the grid.

The resultant forces were calculated for each grid area and their vertical components minus the dead load of the truss and roof sheathing were used to calculate the truss reactions (Figs. 15 and 16) using standard static structural analysis methods.

The leeward side of Model 1 experienced higher roof truss reactions than the windward side for each respective truss. The highest value is for the vertical reaction at Truss *X* (Fig. 14) on the trailing leeward side. The peak reaction for either of the two models was −10 kN. This is almost twice as high as the capacity of a commonly available 18 gauge hurricane tie as reported by Canfield et al. (1991) and 5 times as great as the capacity of a toe-nailed connection using three 16d box nails. This clearly makes the toe-nailed connection inadequate and requires a significant increase in capacity over the use of a single hurricane tie. A possible method of increasing the RTWC capacity would be to incorporate toe nailed connections in addition to hurricane ties. Reed et al. (1997) found that combining the hurricane tie with toe-nails in the same connection increased the capacity of the RTWC to 8.47 kN for one hurricane tie per rafter and 14.35 kN when 2 hurricane ties of the same type were used for each rafter.

Canfield et al. (1991) found that for the majority of tests conducted the failure mode of the hurricane tie connection was tearing of the metal hurricane tie. Therefore, another possible solution would be to increase the thickness of the metal used in the hurricane tie from 18 gauge to 16 gauge or even 14 gauge. Tests could be done to determine which sheet metal gauge the connection would not fail by tearing of the hurricane tie, but rather fail by splitting of the wood members in order to optimize the capacity of the hurricane tie without adding significant cost to the connection.

The hurricane ties mentioned above are available nationwide at common hardware stores for about US$0.60 each. The addition of 2 of these ties to each rafter or to each roof truss support is insignificant to the cost of construction of a new low-rise residential structure.

5. Conclusions

The purpose of the study presented here was to investigate the effect of different building geometry on the forces and pressures that low-rise buildings would experience in a simulated tornado with a swirl ratio comparable to what has been measured and recorded for full-scale tornadoes and to use the measured force and pressure data to judge whether tornado-resistant design for residential structures is feasible instead of basing this on opinion and engineering judgment. In order to achieve these goals the pressures on nine low-rise building models were recorded when the models were subjected to a simulated tornado with a swirl ratio of 2.6 using the Iowa State University's tornado simulator. The study found that the peak pressure coefficients, force coefficient time histories and peak force coefficients vary as a function of eave height, roof pitch, aspect ratio, plan area, and other differences in geometry such as the addition of a “garage” and

modeling of the roof overhang and soffit. These geometric variables also influence the forces and pressures that would need to be resisted by the structure in tornado-resistant design. It appears that the design of the two critical roof connections in residential construction for tornado-resistant design up to and including EF3 tornadoes can be made to be cost-effective by using currently available technology.

Acknowledgment

This research was funded by the National Oceanic and Atmospheric Administration (NOAA) under Award # NA09OAR4600222.

References

ASCE 7-10, 2010. ASCE Standard, Minimum Design Loads for Buildings and Other Structures. American Society of Civil Engineers/SEI, Reston, Virginia

Bluestein, H.B., Golden, J., 1993. A review of tornado observations. In: Church, C., et al. (Eds.), The Tornado: Its Structure, Dynamics, Prediction, and Hazards. American Geophysical Union, p. 79

Brooks, H.E., 2004. On the relationship of tornado path length and width to intensity. Weather and Forecasting 19, 310–319.

Canfield, L.R., Niu, S.H., Liu, H., 1991. Uplift resistance of various rafter-wall connections. For. Prod. J. 41, 27–34.

Church, C.R., Snow, J.T., Baker, G.L., Agee, E.M., 1979. Characteristics of tornado-like vortices as a function of swirl ratio: a laboratory investigation. J. Atmos. Sci. 36, 1755–1776.

Davies-Jones, R.P., 1973. The dependence of the core radius on swirl ratio in a tornado simulator. J. Atmos. Sci. 30, 1427–1430.

Haan, F.L., Balaramudu, V.K., Sarkar, P.P., 2010. Tornado- induced wind loads on a low-rise building. J. Struct. Eng. 136, 106–116.

Haan, F.L., Sarkar, P.P., Gallus, W.A., 2008. Design, construction and performance of a large tornado simulator for wind engineering applications. Eng. Struct. 30, 1146–1159.

Hangan, H., Kim, J.D., 2008. Swirl ratio effects on tornado vortices in relation to the Fujita Scale. Wind Struct. 11, 291–302.

ICC. 2012 International Residential Code. International Code Council, 2012.

Karstens, C.D., Samaras, T.M., Lee, B.D., Gallus , W.A., Finley, C.A., 2010. Near ground pressure and wind measurements in tornadoes. Mon. Weather Rev. 138, 2570–2588.

Lee, W.C., Wurman, J., 2005. Diagnosed three-dimensional axisymmetric structure of the Mulhall tornado on 3 May 1999. J. Atmos. Sci. 62, 2373–2393.

Marshall, T.P., 2002. Tornado damage survey at Moore, Oklahoma. Weather and Forecasting 17, 582–598.

Reed, T.D., Rosowsky, D.V., Schiff, S.D., 1997. Uplift capacity of light-frame rafter to top plate connections. J. Archit. Eng. 4, 156–163.

Sarkar, P.P., Haan, F.L., Gallus, W.A., Le, K., Kardell, R., Wurman, J., 2005. A laboratory tornado simulator: comparison of laboratory, numerical and full-scale measurements. In: Proceedings of the Tenth Americas Conference on Wind Engineering. Baton Rouge, LA.

Sparks, P.R., Hessig, M.L., Murden, J.A., Sill, B.L., 1988. On the failure of single-story wood-framed houses in severe storms. J. Wind Eng. Ind. Aerodyn. 29, 245–252.

Thampi, H., Dayal, V., Sarkar, P.P., 2011. Finite element analysis of interaction of tornadoes with a low-rise timber building. J. Wind Eng. Ind. Aerodyn. 99, 369–377.

TTU, 2004. A recommendation for an Enhanced Fujita Scale. Wind Science and Engineering Center, Texas Tech University, Lubbock, Texas

Wurman, J., 2002. The multiple-vortex structure of a tornado. Weather and Forecasting 17, 473–505.